Supporting Information

Microfluidics Prepared Uniform Conjugated Polymer Nanoparticles for Photo-triggered Immune Microenvironment Modulation and Cancer Therapy

Zhe Wang,[a‡] *Bing Guo,*[b‡] *Eshu Middha,*[b] *Zemin Huang,*[a] *Qinglian Hu,*[*a] *Zhengwei Fu,*[*a] *Bin Liu*[*b]

[a] College of Biotechnology and Bioengineering, Zhejiang University of Technology, Hangzhou 310032, China

[b] Department of Chemical and Bio-Molecular Engineering, National University of Singapore, 117585, Singapore

Corresponding Author

Dr. Qinglian Hu. College of Biotechnology and Bioengineering, Zhejiang University of Technology, Hangzhou 310032, China. Email: huqinglian@zjut.edu.cn;

Prof. Zhengwei Fu. College of Biotechnology and Bioengineering, Zhejiang University of Technology, Hangzhou 310032, China. Email: azwfu@zjut.edu.cn

Prof. Bin Liu. Department of Chemical and Biomolecular Engineering, National University of Singapore, 4 Engineering Drive 4, Singapore, 117585. Email address: cheliub@nus.edu.sg

Experimental Procedures

1. Materials and Characterizations

3,6-Bis(5-bromothiophen-2-yl)-2,5-bis(2-hexyldecyl)pyrrolo[3,4-c]pyrrole-1,4(2H,5H)-dione and 2,5-bis(trimethylstannyl)thiophene were purchased from Derthon. 1,2-Distearoyl-*sn*-glycero-3phosphoethanolamine-*N*-[methoxy(polyethyleneglycol)-2000] (DSPE-PEG_{2000}) and 1,2-distearoyl-*sn*-glycero-3-phosphoethanolamine-*N*-[methoxy(polyethylene glycol)-2000] maleimide (DSPE-PEG_{2000}-MAL) were purchased from Avanti Polar Lipids, Inc. 3-(4,5-Dimethylthiazol-2-*yl*)-2,5-diphenyl tetrazolium bromide (MTT) and tetrahydrofuran (THF) were obtained from Sigma-Aldrich. Thiolated cyclo(Arg-Gly-Asp-D-Phe-Lys (mpa)) peptide (c-RGD) was supplied from GL Biochem Ltd. TRIzol reagent was supplied by Takara (Dalian, China). The ReverTra Ace® qPCR RT Kit and SYBR® Green Realtime PCR Master Mix were obtained from Toyobo (Tokyo, Japan). (RPMI) 1640 medium, fetal bovine serum (FBS), penicillin-streptomycin solution and trypsin-EDTA solution were obtained from Biological Industries (BI). Oligonucleotide primers were supplied by Sangon Biotech (Shanghai, China). APC anti-mouse CD3 antibody, FITC anti-mouse CD4 antibody, APC anti-mouse CD69 antibody and PE-cy7 anti-mouse CD8 antibody were purchased from Bio-legend. Mouse interferon-γ (IFN-γ), interleukin 12p70 (IL-12p70), interleukin 10 (IL-10) and tumor necrosis factor α (TNF-α) ELISA Kits were purchased from Multi Science, Hangzhou, China. All other reagents were used as received. NMR spectra were investigated using a Bruker 500 NMR spectrometer, in which the chemical shifts of both residual solvent peaks and TMS at δ = 0.00 ppm were used as references. Gel permeation Chromatography (GPC) characterization was conducted using an aphenogel GPC column and Waters 996 photodiode detector. Polystyrene with narrow molecular weight distribution was used as the standard, and THF (1.0 mL/min) was used as eluent at 25 ^{o}C. UV-vis test was carried out using a UV spectrometer (Shimadzu Model UV-1700). Dynamic light scattering (DLS) and field emission

transmission electron microscopy (FETEM) were used to investigate the NP size and its, respectively.

2. Synthesis of CP (P0)

A solution of 3,6-bis(5-bromothiophen-2-yl)-2,5-bis(2-hexyldecyl) pyrrolo [3,4-c] pyrrole-1,4 (2H,5H)-dione (108.8 mg, 0.12 mmol), 2,5-bis(trimethylstannyl) thiophene (49.2 mg, 0.12 mmol), $Pd_2(dba)_3$ (2.2 mg, 2.4 μmol) and P(*o*-tol)$_3$ (5.8 mg, 19.2 μmol) in toluene (15 mL) was vigorously stirred in a Schlenk tube at 100 ^oC under argon atmosphere for 24 h. When the reaction was finished, 15 mL of toluene was added in the Schlenk tube to dilute the viscous polymer solution. The polymer solution was slowly precipitated into cold acetone (400 mL). The precipitate was collected by filtration and underwent extensive washing using acetone. The crude product was completely dissolved in chloroform and the resultant polymer solution was filtered through a short silica column, and further concentrated by rotary evaporation. Finally, the concentrated polymer solution was dropwise precipitated in excess cold acetone and filtered to collect the powders. The obtained crude powders were dried in vacuum oven to yield product polymer P0 as a dark solid (82 mg, yield 82%). ^1H NMR (500 MHz, $C_2D_2Cl_4$, 100 ^oC) δ 8.95-8.86 (m, 4H), 7.51-7.00 (m, 2H), 4.10 (b, 4H), 2.06 (br, 2H), 1.52-1.35 (m, 48H), 0.94 (br, 6H); GPC (THF, polystyrene standard), M_n: 3.4 $\times 10^4$ g/mol; M_w: 7.5 $\times 10^4$ g/mol, PDI: 2.2.

3. Fabrication of Microfluidic Glass Mixer

The coaxial flow microfluidic glass capillary mixer was assembled by using two round glass capillaries of diameter 1 mm (for outer) and 0.7 mm (for inner), teflon tubings and fittings from Chemikalie Pte Ltd. The inner round capillary was pulled using a micropipette puller (Sutter Instruments, P-97) to produce a tapered end. The tapered end was then enlarged to 100 μm using abrasive paper. Teflon tubing was used to connect the glass capillary device to respective syringes controlled by syringe pumps. The inner glass capillary was inserted into outer glass capillary with a side hole in teflon tubing. The outer glass capillary is connected to

a plastic monoject syringe through Teflon tubing and fittings for the supply of water. The pump used for the water supply was a Chemyx Nexus-3000 pump and the organic phase was injected by using a Chemyx Fusion-200 pump.

4. Calculation of Reynolds Number and Flow Velocity

The total flow rate in the system was varied from 1.1 mL min^{-1} to 16.5 mL min^{-1}. The relation between flow velocity (u) and volumetric flow rate (Q) is defined by Equation S1.

$$u = \frac{4Q}{\pi D_i} \quad \text{(S1)}$$

where D_i is the inner diameter of the pipe (1 mm)

Re in the system was varied on the basis of the total flow rate using the following Equation S2.

$$Re = \frac{\rho u L}{\mu} \quad \text{(S2)}$$

where μ represents the viscosity of fluid, ρ represents the density of the fluid and L is a characteristic linear dimension (m). For circular pipe, characteristic linear dimension is the same as the hydraulic diameter (inner diameter of pipe). Equation S4 represents the relation between Re and flow rate.

$$Re = \frac{4\rho Q}{\pi \mu} \quad \text{(S3)}$$

5. BCA Assay

The NP surface c-RGD quantitation was conducted using BCA assay kit (Beyotime Biotechnology, China) according to the reference.[1] The free c-RGD concentration in NP suspension was analyzed and the RGD labeling efficiency accordingly calculated.

6. Photothermal Performance Evaluation

The different concentrations of P0 NPs (10, 20, 50 μg/mL) were continuously irradiated with an 808 nm NIR laser (1.0 and 2.0 W cm^{-2}) for 10 min using pure water as the control,

respectively. The temperature changes were recorded every 30 s. For anti-photo bleaching performance, the temperature changes of solution containing 50 μg/mL P0 NPs were measured during three circles of heating and cooling process. In each heating-cooling circle, the photothermal laser was applied to irradiate the CP NP suspension for 10, then the laser was turned off, and the suspension was naturally cooled down to ambient temperature.

7. Cellular uptake.

To investigate the cellular uptake of P0 NPs and P0RGD NPs, the fluorescent PFBT molecules were co-encapsulated with P0 to prepare P0-PFBT NPs and P0-PFBT RGD NPs (the mass ratio of P0:PFBT=1:2). 4T1 cells (30×10^4 cells/well) were seeded into 6-well plates with 2 mL of medium. After 24 h, the media were replaced with RPMI 1640 medium containing 10 μg/mL P0-PFBT NPs or P0-PFBT RGD NPs. After 24 h incubation, the cells were washed three times with PBS. The fluorescence images were acquired by Fluorescence microscope (NIKON ECLIPSE Ti2, Japan). For quantitative analysis, 4T1 cells were harvested and quantitatively determined by flow cytometry (BD FACS Melody，USA).

8. In Vitro Cytotoxicity Study

RAW264.7 cells (1×10^4 cells per well) were severally seeded into 96-well plates and further cultured overnight (5% CO_2, 37 °C). Next, different concentrations of P0 NPs and P0RGD NPs were respectively added to culture media and incubated for 24 h. At the flowing, the cells were treated with PBS washing for three times and 100 μL of 0.5 mg/mL MTT working solution was added into each well at 37 °C for 4 h. For PTT treatment, the cells were treated with laser irradiation (808 nm, 2.0 W cm^{-2}, 10 min). After overnight culture, the cells were further incubation with MTT solution. The MTT solution was removed and DMSO (100 μL) was subsequently added to totally dissolve the formed formazan crystals. Then the absorbance was measured at 490 nm using a microplate reader (Themo Multiscan MK3, USA). Cell viability was calculated according to the ratio of absorbance value of the cells

cultured with NP suspensions divided by the absorbance value of the cells only treated with culture medium.

9. RT-qPCR analysis and Enzyme-linked immunosorbent assay

To evaluate the performance of PTT treatment on immune response of RAW264.7 cells, the cells were treated with 1 and 10 μg/mL P0RGD NPs for 24 h. For PTT treatment, the RAW264.7 cells were irradiated with 808 nm laser (2.0 W cm^{-2}) for 10 min. After overnight culture, the mRNA expressions of *IL-1β, IL-6, IL-12, TNF-α* and *CXCL-1* were investigated *via* RT-PCR.

The peritoneal macrophage was purified according to the conventional protocol. For peritoneal macrophages activation assay, 0.1 μg/mL of CP NPs was chosen to incubate with mouse peritoneal macrophage for 24 h and then irradiated with 808 nm laser (2 W cm^{-2}) for 10 min. PBS as a control. The mRNA expression level of TNF-α, IL-1β, IL-6, CXCL-1, IL-12, iNOS, IL-10, Arg-1 and CD206 were measured by semi-quantitative real-time PCR analysis (RT-qPCR) according to the instructions, meanwhile, the amount of cytokines IL-1β, IL-6 and TNF-α in the supernatant was tested using mouse enzyme-linked immunosorbent assay (ELISA) kits according to the manufacturer's instructions.

10. Detection of Cytokines in Tumor Tissue of Mice

The 4T1 xenograft tumor model was established with subcutaneous injection of 4T1 cells (1×10^6) on the right flank of the mice to reach about 100 mm^3 in five different groups (n = 8 in each group), which were underwent different treatments: Only PBS (i), P0 NPs (ii), P0RGD NPs (iii), P0 NPs + laser (iv), P0RGD NPs + laser (v). The mice were injected with 100 μL PTT nanoparticles solution (2 mg/kg BW) through tail vein with every three day for 5 times and the control group received PBS at the same amount. For PTT treatment, the mice were exposed to 808 nm laser irradiation (2 W cm^{-2}) for 20 minutes after intravenous injection for 8 hour. Five days after last laser treatment, the tumors excised from mice were cut into small pieces and lysed with collagenase I (1mg/ml) for 2 h. The single-cell suspension was

prepared and the protein levels of IL-10 and IL-12p70 were measured with ELISA by following manufacturer's protocol.

11. Histological Studies

Five days after last laser treatment, the last mice were sacrificed. At the following, tumors and major organs (liver, spleen) of mice were harvested for histology analysis. The hematoxylin and eosin (H&E) staining was conducted according to a standard protocol as follows: the liver and spleen tissues were fixed using formalin solution (4%), processed into paraffin, and sectioned to a thickness of 5 μm. Finally, the slices were studied using a Leica microscope (Leica DFC450C).

12. Serum Biochemistry Assay and Complete Blood Count.

Five days after last laser treatment, all mice in the above-mentioned five different groups were sacrificed. At the same time, mice blood was carefully collected and characterized with an automated hematology analyzer.

Table S1. Variation of Re in the pipe due to change in flow rate (mL min^{-1})

Flow Rate (mL min^{-1})	Reynolds No
1	21.2
2	42.4
3	63.6
5	106.0
7	148.4
10	212.2
15	318.2

Table S2. Primers used for the quantitative PCR analysis

Gene	sequence
IL-1β	Forward 5'-CCAACAAGTGATATTCTCCATGAG-3'
	Reverse 5'-ACTCTGCAGACTCAAACTCCA-3'
IL-6	Forward 5'-CTCTGCAAGAGACTTCCATCC-3'
	Reverse 5'-GAATTGCCATTGCACAACTC-3'
IL-12	Forward 5'GGAAGCACGGCAGCAGAATA-3'
	Reverse 5'AACTTGAGGGAGAAGTAGGAATGG-3'
TNF-α	Forward 5'-GTCTACTGAACTTCGGGGTGAT-3'
	Reverse 5'-GGCTACAGGCTTGTCACTCG-3'
CXCL-1	Forward 5'ACTGCACCCAAACCGAAGTC-3'
	Reverse 5'TGGGGACACCTTTTAGCATCTT-3'
CD206	Forward mouse IL-10 5'-GCTCTTACTGACTGGCATGAG-3'
	Reverse 5'CGGAATTTCTGGGATTCAGCTTCG-3'
	Forward 5'ACTACTGCTGGTGGTGACAA-3'
iNOS	Reverse 5'GAAGGTGTGGTTGAGTTCTCTAAG-3'
	Forward 5'CGCCTTTCTCAAAAGGACAGC-3'
Arg-1	Reverse 5'CAGCTCTTCATTGGCTTTCAC-3'
Gapdh	Forward 5'GTGGCAAAGTGGAGATTGTTG-3'
	Reverse 5'AGTCTTCTGGGTGGCAGTGAT-3'

Table S3. Photothermal conversion efficiency of organic and inorganic nanoparticles

Nanoparticles	Photothermal conversion efficiency (%)	Laser wavelength (nm)
P0 NPs in this study	40	808
P1 NPs[1]	30.1	1064
SPN1-C[2]	37	808
Dopaminemelanin Colloidal nanospheres[3]	40	808
Au@polymer nanoparticles (NPs) [4]	23	808
MCH NPs[5]	20.98	808
Fe_3O_4 CNPs[6]	20.8	808

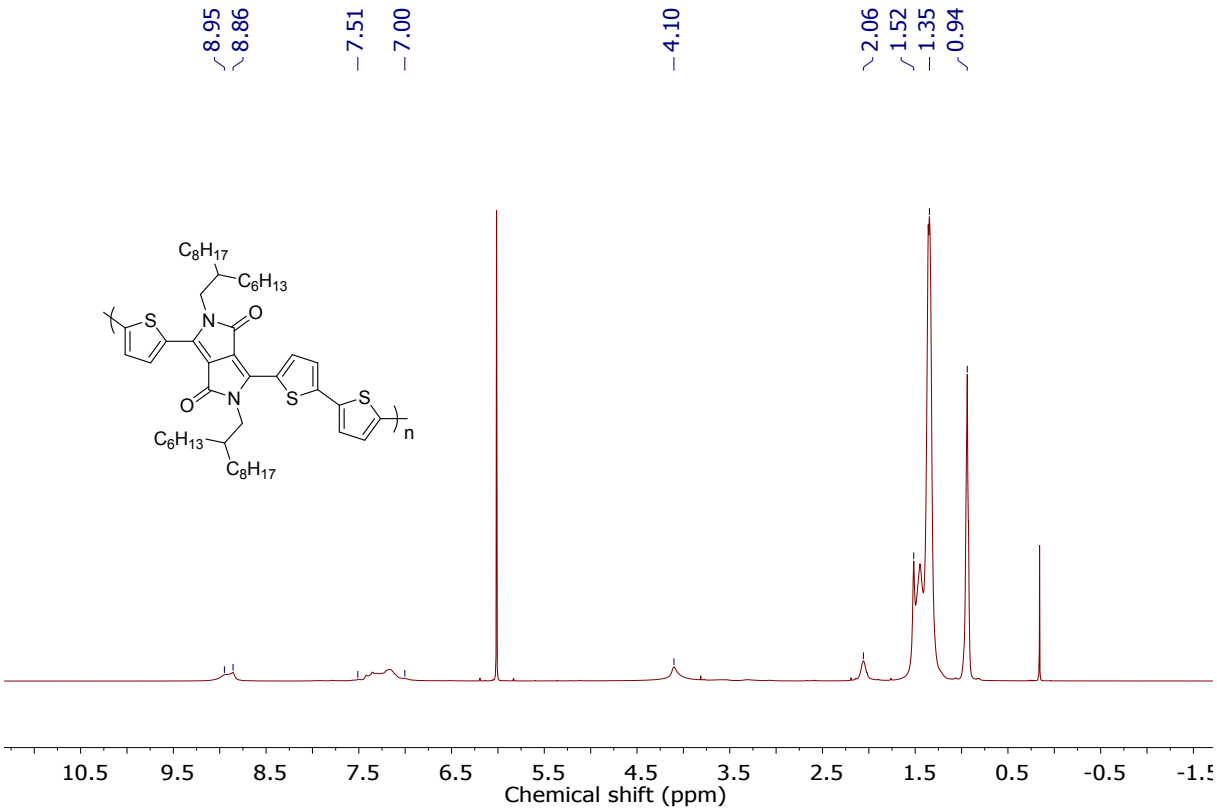

Figure S1. ^1H NMR spectrum of P0 in $C_2D_2Cl_4$ at 100 °C.

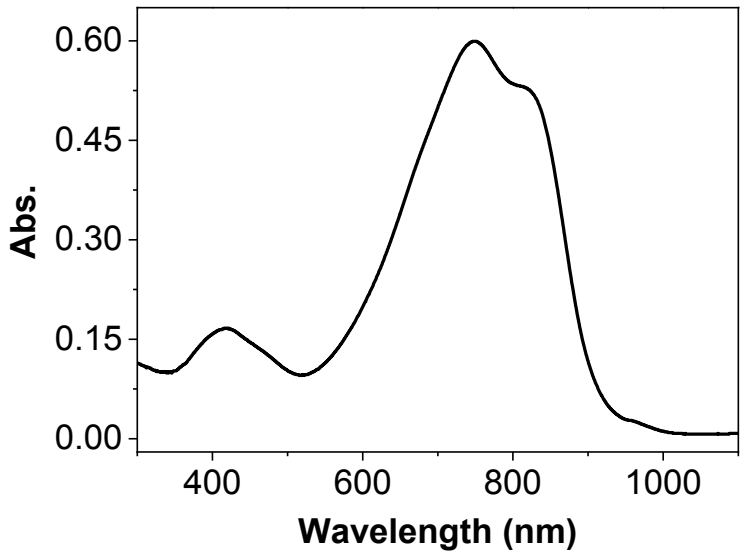

Figure S2. UV/vis spectrum of P0 NPs in water.

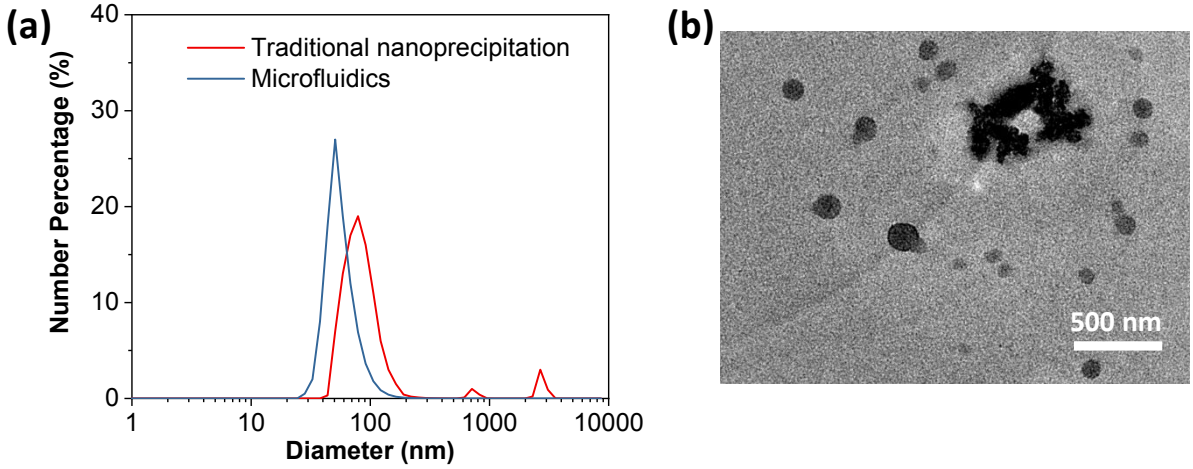

Figure S3. (a) Comparison of number size distribution of P0 loaded DSPE-mPEG NPs synthesized by using traditional nanoprecipitation and microfluidic glass capillary; (b) TEM images of P0 NPs prepared by traditional nanoprecipitation.

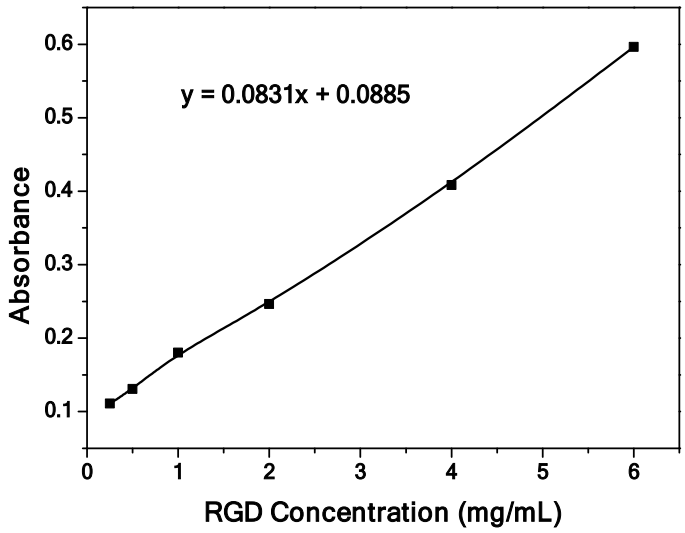

Figure S4. The 562 nm absorbance of BCA assay kit in the presence of c-RGD standard samples with different concentrations.

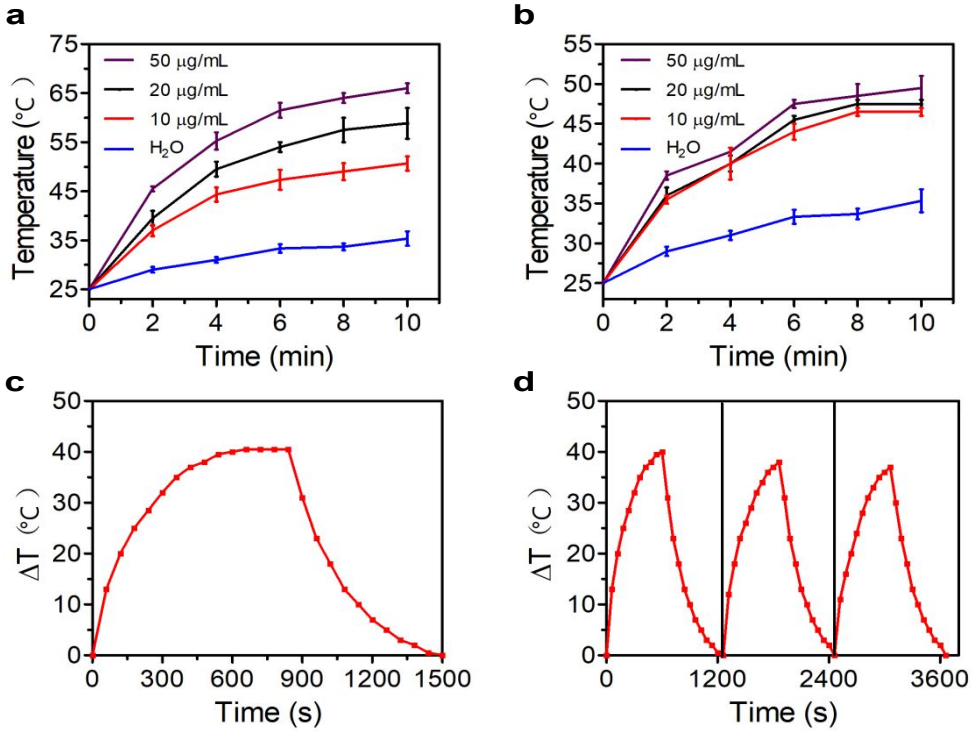

Figure S5. Photothermal performance evaluation of P0 NPs with different concentrations under continuous 10 min of 808 nm laser irradiation at power of (a) 2.0W cm^{-2} and (b) 1.0 W cm^{-2}. (c) The record of the photothermal response of P0 NP suspension with laser irradiation (808 nm, 2.0 W cm^{-2}) and the cooling process. (d) Temperature curves of P0 NPs in water under laser irradiation for 3 cycles (808 nm, 2 W cm^{-2}, 10 min with irradiation and 10 min without irradiation for each cycle).

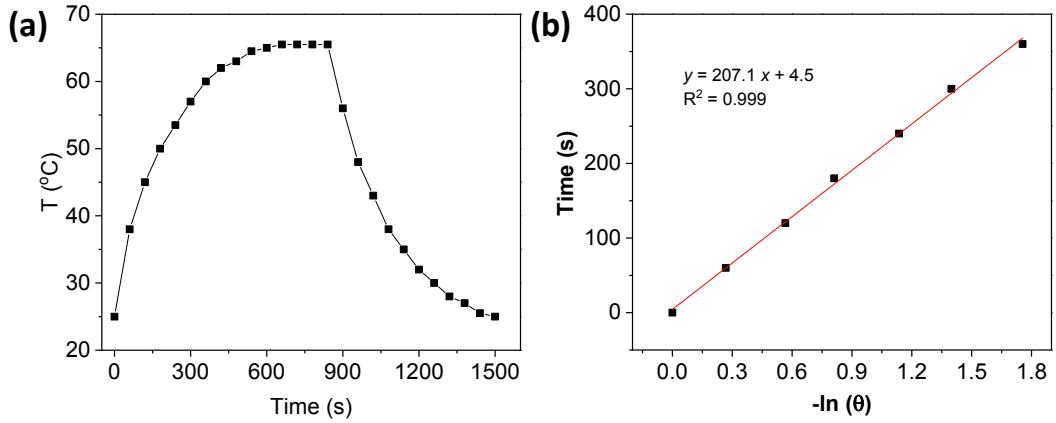

Figure S6 (a) Temperature changes of P0 NPs under 808 nm laser irradiation (2 W cm^{-2},) and cooling process after the photothermal treatment; (b) The time constant for the system heat transfer, calculated by the linear cooling time versus the negative natural logarithm of the driving force temperature in the system. ($\theta = (T-T_{sur})/(T_{max}-T_{sur})$, where T is the temperature at different cooling time point, T_{sur} (25 °C) is the environmental temperature, T_{max} (65.5 °C) is the equilibrium temperature under 808 nm laser irradiation.

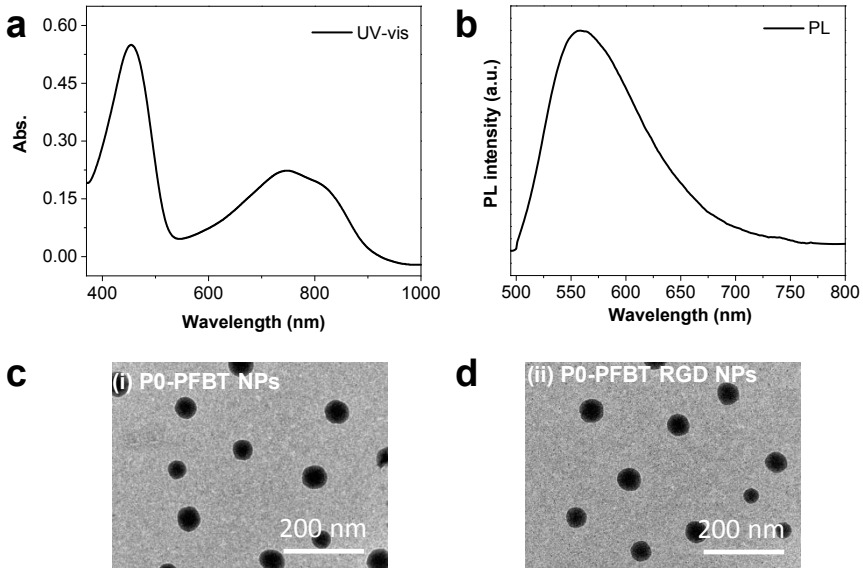

Figure S7. The UV (a) and PL (b) spectra of P0-PFBT NPs. TEM images of P0-PFBT NPs (c) and P0-PFBT RGD NPs (d).

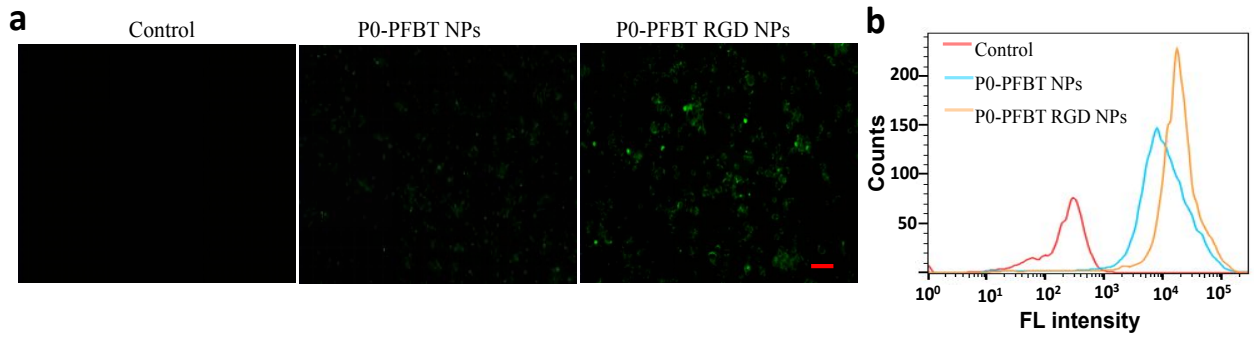

Figure S8. The cellular uptake of P0-PFBT NPs and P0-PFBT RGD NPs in 4T1 cells. (a) Fluorescence images after 24 h incubation with 10 μg/mL P0NPs or P0RGD NPs. Green represents the fluorescence of NPs (scale bar, 100 μm). (b) The uptake analysis of 4T1 cells by flow cytometry.

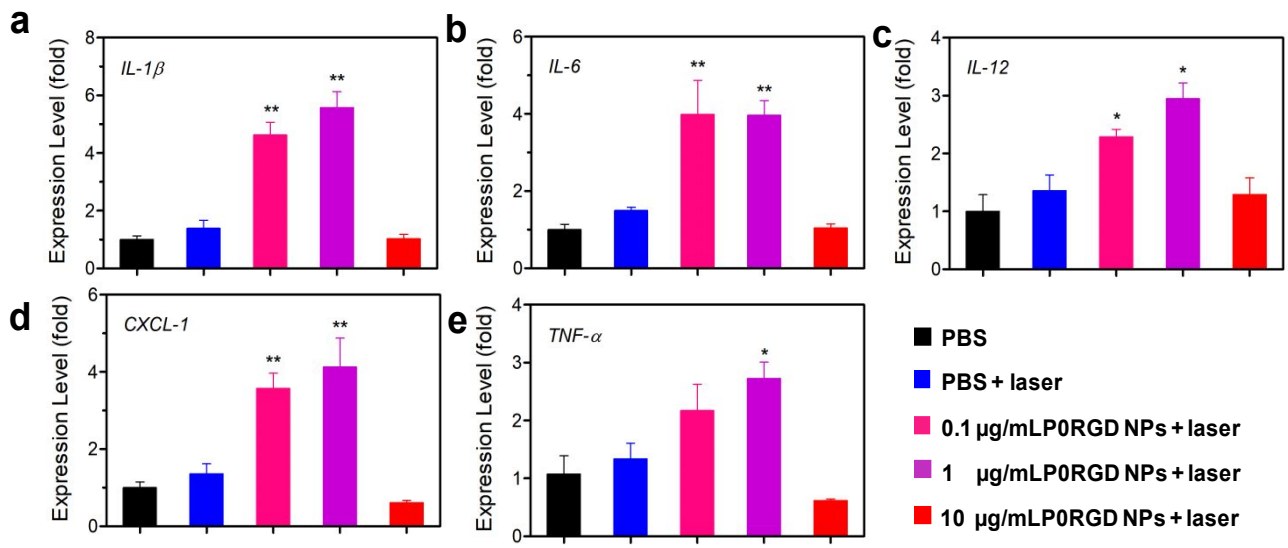

Figure S9. The mRNA expressions of (a) IL-1β, (b) IL-6, (c) IL-12, (d) TNF-α, (e) CXCL-1 in RAW264.7 cells quantitatively tested by real-time PCR analysis after 24 h incubation with 0.1, 1 and 10 μg/mL P0RGD NPs with and without photothermal laser irradiation (808 nm, 2 W/cm^2). All data are shown as means±SEM (n = 6, *p < 0.05 and **p < 0.01 with control groups ascomparison).

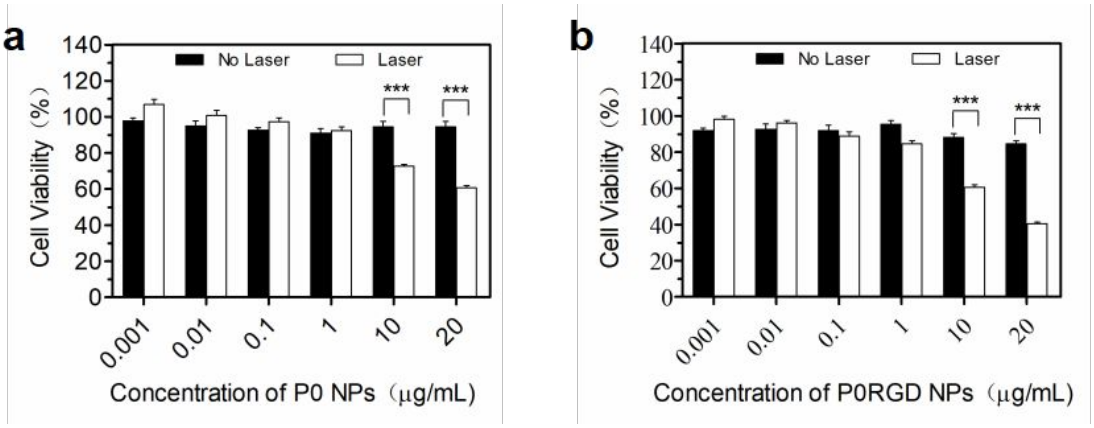

Figure S10. In vitro raw 264.7 cell viability of P0 NPs (a) and P0RGD NPs (b) at different concentrations after 24 h incubation with or without out laser irradiation for 10 min. Laser parameters: 808 nm; laser power, 2 W cm^{-2}). Data were expressed as means ± SEM (n = 6, ***$p < 0.001$ compared with control group).

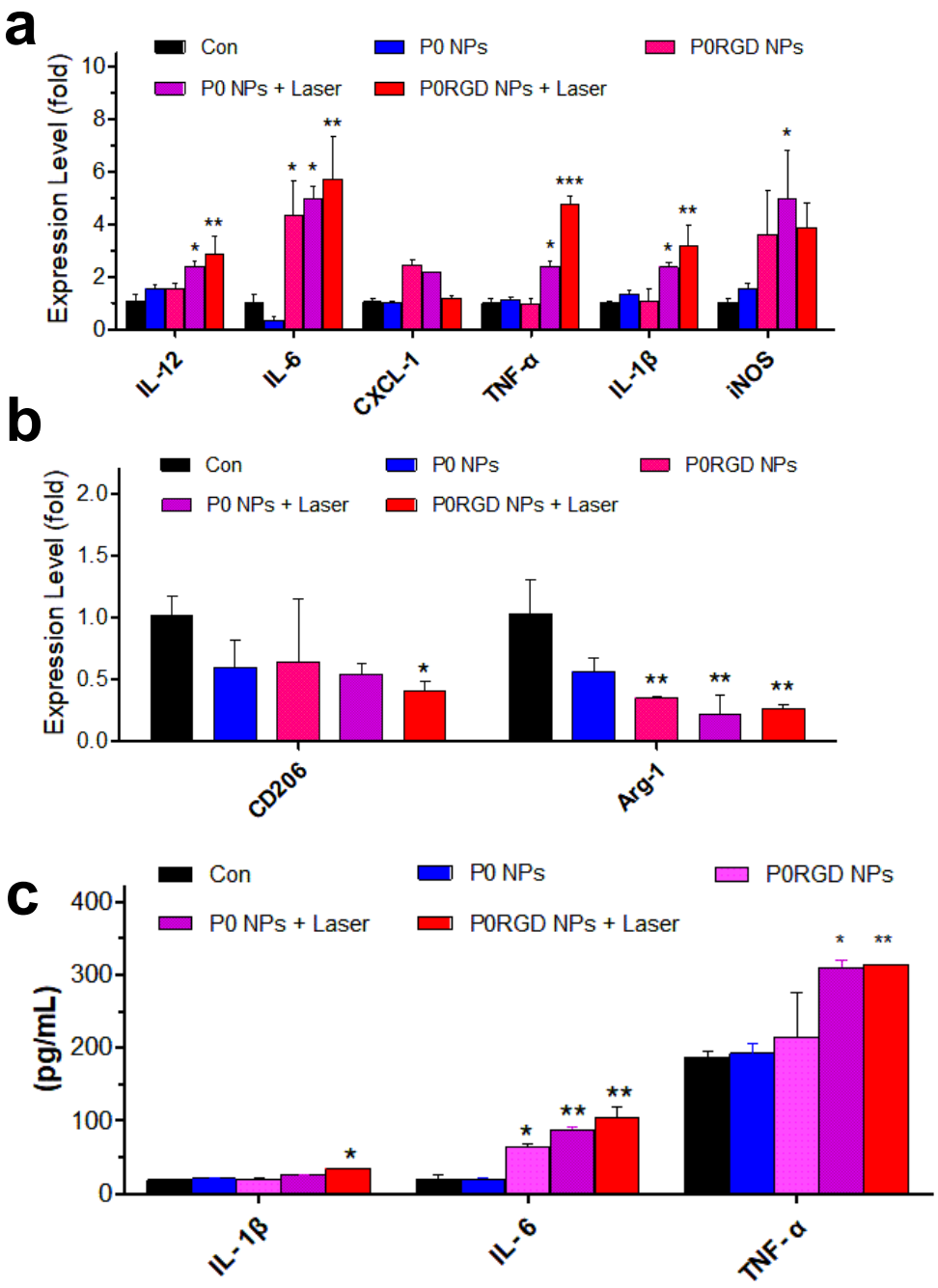

Figure S11. The RT-qPCR analysis of M1- and M2-macrophage-related markers in peritoneal macrophages (a,b) and release of pro-inflammatory cytokines of IL-1β, IL-6 and TNF-α in serum by using ELISA assay (c) after 24 h incubation with P0 NPs and P0RGD NPs with and without photothermal laser irradiation (808 nm, 2 W/cm2). All data are shown as mean ± SEM (n =3, *p < 0.05, **p < 0.01 and ***p < 0.001compared with control group).

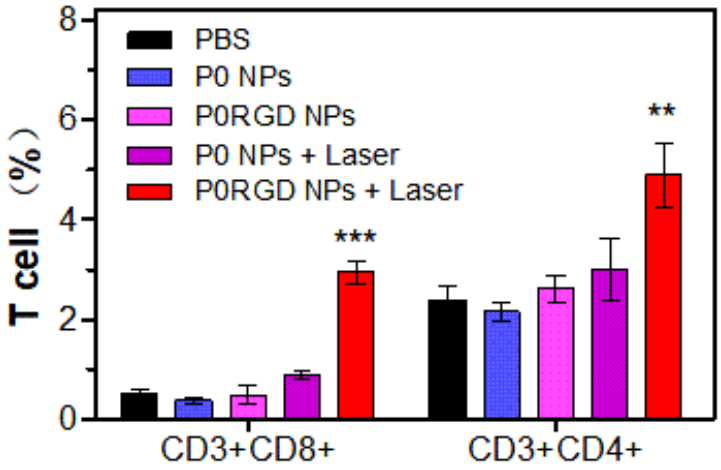

Figure S12. Proportions of tumor-infiltrating CD8+ killer T cells regulatory T cells according to data in Figure 4c and 4d.

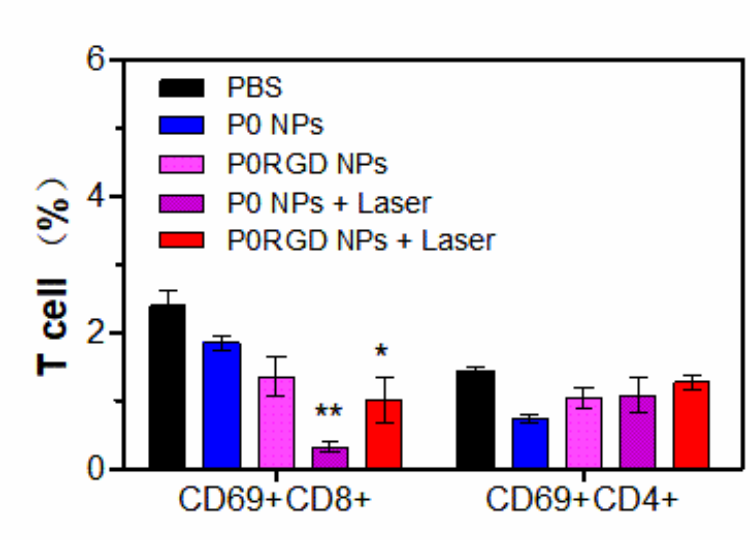

Figure S13. The populations of activated CD8+ T cells (CD8+CD69+) and CD4+ T cells (CD4+CD69+) in the spleen after different treatments according to data in Figure 5c and 5d. Data are presented as the mean±SEM. Error bars are based on triplicated experiments.

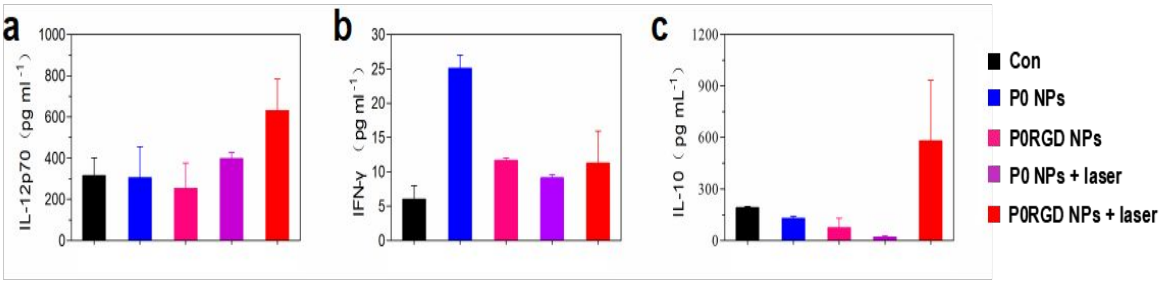

Figure S14. The levels of (a) IL-12p70 and (b) IFN-γ and (c) IL-10 in the tumors after five days of last treatments. Three mice were measured in each group. Data were expressed as means ± SEM (n = 3).

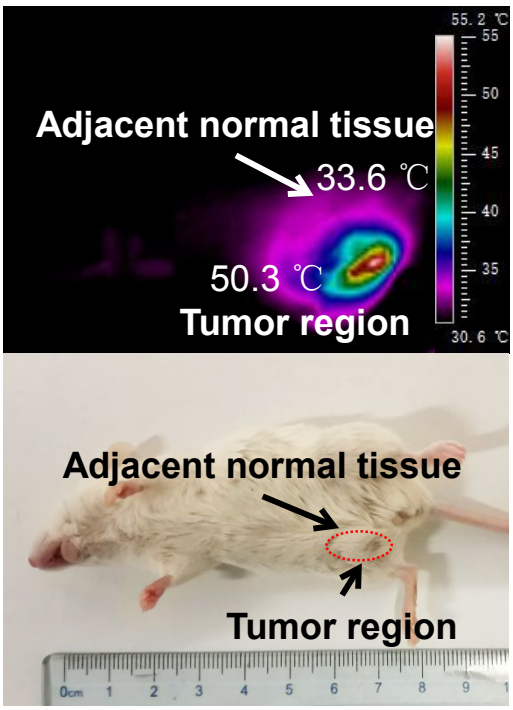

Figure S15. Infrared thermal images of mice tumor and adjacent normal tissue after photothermal treatment for 20 min (808 nm, 2 W/cm^2), after 8 h post-injection with P0RGD NPs (2 mg/Kg)

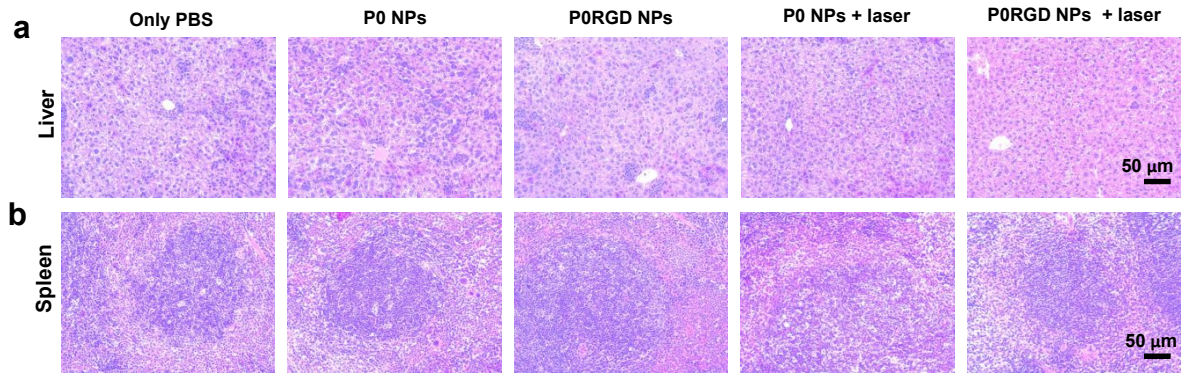

Figure S11

Figure S16. H&E staining of liver (a) and spleen tissues (b) after five days of last treatments. Scale bar : 50 μm.

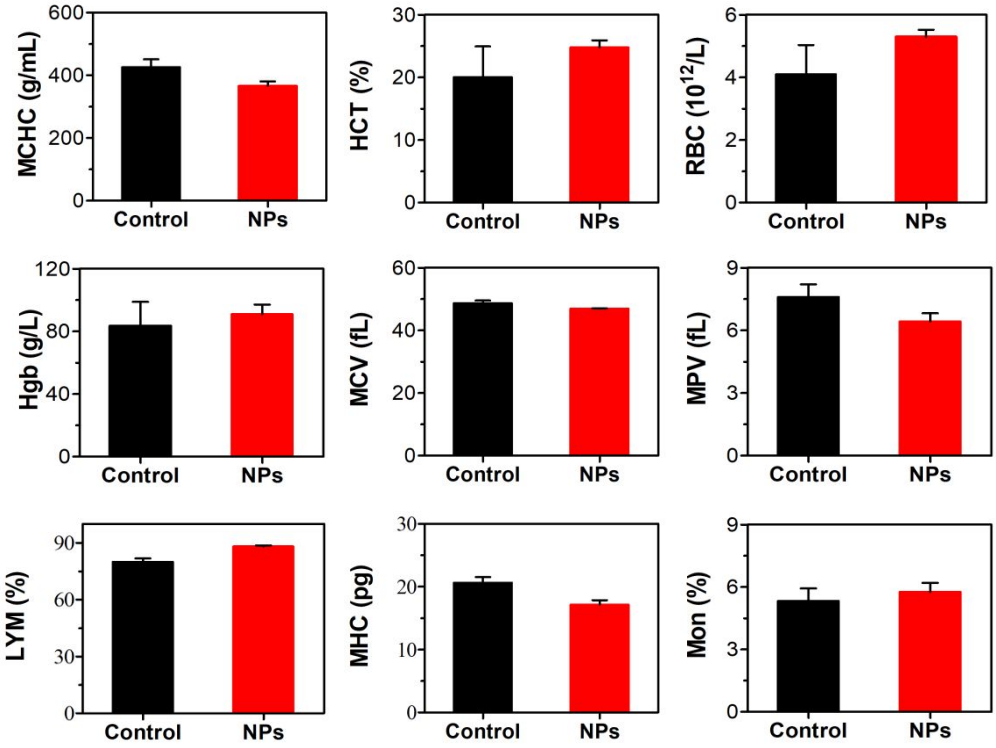

Figure S17. Hematology and blood biochemical assay of mice at 19 d post injection of P0RGD NPs. mean corpuscular hemoglobin concentration (MCHC); hematocrit (HCT); number of red blood cells (RBC); concentration of hemoglobin (HGB); mean corpuscular volume (MCV); mean platelet volume (MPV); lymphocyte (LYM); mean hemoglobin concentration (MHC); monocytes (Mon).

References

(1) Guo, B.; Sheng, Z. H.; Hu, D. H.; Liu, C. B.; Zheng, H. R.; Liu, B. Through Scalp and Skull NIR-II Photothermal Therapy of Deep Orthotopic Brain Tumors with Precise Photoacoustic Imaging Guidance. *Adv. Mater.* **2018,** *30*, e1802591.

(2) Zhen, X.; Xie, C.; Jiang, Y.; Ai, X.; Xing, B.; Pu, K. Semiconducting Photothermal Nanoagonist for Remote-Controlled Specific Cancer Therapy. *Nano Lett.* **2018,** *18*, 1498-1505.

(3) Liu, Y. L.; Ai, K. L.; Liu, J. H.; Deng, M.; He, Y. Y.; Lu, L. H. Dopamine-Melanin Colloidal Nanospheres: An Efficient Near-Infrared Photothermal Therapeutic Agent for In Vivo Cancer Therapy. *Adv. Mater.* **2013,** *25*, 1353-1359.

(4) Huang, C. C.; Liu, T. M. Controlled Au-Polymer Nanostructures for Multiphoton Imaging, Prodrug Delivery, and Chemo-Photothermal Therapy Platforms. *ACS Appl. Mater. Interfaces* **2015,** *7*, 25259-25269.

(5) Zhang, Y.; Wang, L.; Liu, L.; Lin, L.; Liu, F.; Xie, Z. G.; Tian, H. Y.; Chen, X. S. Engineering Metal-Organic Frameworks for Photoacoustic Imaging-Guided Chemo-/Photothermal Combinational Tumor Therapy. *ACS Appl. Mater. Interfaces* **2018,** *10*, 41035-41045.

(6) Huang, C. C.; Chang, P. Y.; Liu, C. L.; Xu, J. P.; Wu, S. P.; Kuo, W. C. New Insight on Optical and Magnetic Fe_3O_4 Nanoclusters Promising for Near Infrared Theranostic Applications. *Nanoscale* **2015,** *7*, 12689-12697.